Applied Thermal Engineering 219 (2023) 119586

Contents lists available at ScienceDirect

Applied Thermal Engineering

journal homepage: www.elsevier.com/locate/apthermeng

Ground source heat pump driven by reciprocating engine firing biomethane from wastewater treatment plant sludge in a cogeneration for district heating and cooling. A case study in Spain

L. Serrat [a], J.I. Linares [a,*], M.M. Cledera [a,b], C. Morales [a,b], K. Hueso [a,b]

[a] Rafael Mariño Chair in New Energy Technologies, ICAI School of Engineering, Comillas Pontifical University, Alberto Aguilera, 25 - 28015 Madrid, Spain
[b] Institute for Research in Technology (IIT), ICAI School of Engineering, Comillas Pontifical University, Alberto Aguilera, 25 - 28015 Madrid, Spain

ARTICLE INFO

Keywords:
Biomethane
Wastewater treatment plant
Ground source heat pump
Cogeneration reciprocating engine

ABSTRACT

Wastewater treatment plants are a key facility in municipalities to reach the required water quality before returning to the environment. Their energy consumption constitutes the most critical cost in their operation, although sludge produced in the treatment can be fed into an anaerobic digester to produce biogas. Such biogas is usually burnt into a cogeneration reciprocating engine that produces power injected into the grid and heat to maintain the required temperature in the digester. This energy recovery technique also avoids direct methane emissions from the biogas to the atmosphere. An alternative energy recovery of the sludge is proposed in this paper, seeking to cover both the winter and summer thermal demands of the municipality whose wastewater is treated by the plant.

A district heating and cooling network is assumed to be available in the municipality, whose demand will be met (total or partially) by the proposed system. The biogas production has been assessed from a large number of wastewater treatment plants in Spain. This fuel will be upgraded to biomethane to inject eventual surplus generation into the natural gas grid. The hourly thermal demand is estimated from a self-elaboration expansion of annual expressions given in Spanish regulations. A high insulation level in the dwellings of the municipality is assumed to reach the maximum thermal demand coverage level. Underfloor heating and cooling is used as final air conditioning system. The conversion is carried out by supplying the biomethane to a cogeneration reciprocating engine, whose power output drives a ground source heat pump and its recovered heat is used for the thermal conditioning of the biogas digester as well as for heating in winter.

The results show that for a 50,000 inhabitants treatment plant, the thermal demand coverage percentage ranges from 28 % to 51 % and the levelized cost of heating and cooling from 38 to 65 €/MWh$_{th}$. Generally, the lowest cost is reached in zones with an intermediate coverage percentage. Even with high insulation dwellings and high-efficiency systems, the thermal demand coverage percentage is low. This suggests that biomethane production from all the entire municipality can be devoted to meet a selected district's complete demand, built with high standards. This district might be focused on social dwellings.

1. Introduction

The building sector accounts for more than a third of the global energy consumption, with an expected demand growth of 50 % by 2050. The share in the energy mix of residential areas is 40 %, being the most significant fraction of this consumption for heating and cooling demands [1]. Moreover, this sector contributes to global warming, generating 36 % of global greenhouse gases [2]. To reduce these numbers, the European Union promotes different energy policies, including strategies to develop new infrastructures to reduce greenhouse gas emissions [3], and to promote the bioeconomy, and circular economy [4]. In this sense, district heating and cooling networks (DHCN) are revealed as an effective technology, including waste heat and renewable resources [5]. More than 5000 DHCN are currently operating in Europe, covering over 10 % of the demand [2]. Some of them use cogeneration to supply thermal energy and power to the final users. These cogeneration units can be conventional using industrial steam turbines [6] or more advanced, fuelled with renewable sources such as biogas from landfills [7] and wastewater treatment plants [8], or solid biomass [9].

* Corresponding author.
E-mail address: linares@comillas.edu (J.I. Linares).

https://doi.org/10.1016/j.applthermaleng.2022.119586
Received 14 January 2022; Received in revised form 24 October 2022; Accepted 27 October 2022
Available online 1 November 2022

Nomenclature

Symbol	Meaning Units
A	Conditioned area m^2
BTC	Building Technical Code
C_0^F	Annual cost of biomethane at zero year €
C_0^P	Annual cost for powering the pumps of the DHCN at zero year €
C_0^M	Annual cost of maintenance at zero year €
CELF	Constant escalation levelization factor p.u.
CHP	Combined heat and power
COP	Coefficient of performance (for use in winter) p.u.
Cr	Reduction coefficient p.u.
CRF	Capital recovery factor p.u.
CSI	Climate severity index p.u.
ΔTk	Hourly temperature difference °C
δ	Auxiliary coefficient given in Eq. (14) 1/K
$\dot{D}_j$	Hourly absolute demand kWth/m^2
DD	Average degree-days °C
DHCN	District heating and cooling network
E	Electrical energy produced per year MWhe
EER	Energy efficiency ratio (for use in summer) p.u.
EF	Engine fuelling kWth
EPI	Energy performance index p.u.
$\dot{F}_S$	Biomethane consumption in summer kWth
$\dot{F}_W$	Biomethane consumption in winter kWth
FG	Thermal energy released in the flue gases kWth
GD	Thermal energy exchanged with the ground kWth
GI	Grid injection kWth
GIS	Geographical information system
GP	Gross production kWth
GSHP	Ground source heat pump
HMD	Highest met demand
HPN	Thermal energy exchanged with the DHCN kWth
HPW	Power produced by the engine and consumed by the heat pump kWe
HP0	Coefficient for heat pump investment €
HP1	Coefficient for heat pump investment kWth
η_e	Electrical efficiency p.u.
η_V	Thermal efficiency p.u.
IMD	Intermediate met demand
INVHP	Investment of heat pump €
INVRE	Investment of cogeneration reciprocating engine €
j	Counter index
LCOHC	Levelized cost of heating and cooling €/MWhth
LHV	Lower heating value kWh/Nm3
LMD	Lowest met demand
MD	Met thermal demand kWhth
M0	Coefficient for maintenance costs [$€/(MWh_e \bullet kW_e^{0.199})$
N	Equivalent inhabitants
NBP	Net biomethane production kWhth/day
ND	District heating and cooling network demand kWhth
Nd	Number of days in the season day
Nm	Number of months in the season day
Ny	Life span of the project year
oh	Overall hours hour
PMW	Power consumed by the pumping system kWe
PV	Photovoltaic
$\dot{Q}_{HA}$	Heating thermal power available kWth
$\dot{Q}_{CA}$	Cooling thermal power available kWth
$\dot{Q}_{cond}$	Capacity of heat pump kWth
$\dot{Q}_{DHCN}$	Heat exchanged with the district heating and cooling network kWth
ρ	Auxiliary coefficient given in Eq. (13) m^2/kWth
rk	Global hourly radiation over horizontal surface kWth/m^2
R2	Coefficient of determination of a regression p.u.
rn	Nominal escalation rate p.u.
Rs	Ratio of RD (average value from the entire stock of reference buildings) to the reference demand of the 10-th percentile of such stock p.u.
RAD	Average accumulated global radiation over horizontal surface kWth/m2
RD	Reference specific demand kWhth/m^2
RD^a	Actual specific reference demand kWhth/m^2
$\dot{RD}_j$	Corrected hourly specific reference demand kWth/m^2
$\dot{RD}_j^*$	Hourly specific reference demand (before correction) kWth/m^2
RE	Reciprocating engine
RE0	Coefficient for reciprocating engine investment €
RE1	Coefficient for reciprocating engine investment €/kWe
RH	Recovered heat kWth
RHN	Recovered heat to the DHCN kWth
RHD	Recovered heat to the digester kWth
SC	Self-consumption kWth
SCB	Self-consumption of biomethane kWhth/day
Tb	Base temperature to calculate degree-days °C
Tk	Hourly ambient temperature °C
TDCP	Thermal Demand Coverage Percentage %
$\dot{W}$	Power produced by cogeneration reciprocating engine at design point kWe
$\dot{W}_p$	Power consumption of the pumps of the district heating and cooling network kWe
wacc	Weighted average capital cost p.u.
WSI	Winter severity index p.u.
WWTP	Wastewater treatment plant

Biogas is called to play a vital role in the decarbonizing economy. Recently, the European Union has identified it as a substitute for Russian natural gas, with a global potential of 35 bcm in 2030 [10]. Biogas is a renewable gas generated from the natural decomposition of anaerobic digestion by microorganisms of organic matter from several feedstocks (municipal solid wastes [7], agricultural and residue [11], or sewage sludge [12]). Its main components are methane and carbon dioxide, with a volumetric composition between 50 % and 65 % and 35 % to 50 %, respectively, along with impurities such as hydrogen sulphide, siloxanes, steam, and ammonia [13]. Anaerobic digestion of sludge from wastewater treatment plants (WWTP) arose interest as a viable resource a long time ago [14], setting out the generation of thermal energy and power towards DHCNs [15]. WWTPs are facilities in which water contaminated by human use, is subjected to various physical, chemical, and/or biological treatments to remove part of said contamination and safely discharge it back into the natural environment [16]. Although improvements in the energy efficiency of WWTPs have been implemented over the years, they are considered large energy consumers. In fact, it is estimated that 40 % of the total cost of operation corresponds to the energy use [17]. In studies such as that of Longo *et al.* [18], the biological treatments are classified as the largest energy consumers, consisting of 8.4 MWh_{th} for each m^3 of water treated and 16 MWh_{th} for the treatment of sludge. However, there are energy-generating treatment phases in WWTPs, such as anaerobic digestion [19], which produce biogas. WWTPs cease to be seen exclusively as strictly environmental plants to begin to be understood as energy generators

[20]. Thus, anaerobic digestion plays a fundamental role in energy recovery through the WWTP processes [21]. Authors such as Silvestre *et al.* [17] estimate that, nominally, between 39 % and 79 % of the energy requirements of a WWTP can be recovered with the biogas generated, even reaching surplus to be used for other purposes, with energy and environmental benefits as shown by Venkatesh *et al.* [22].

The use of biogas after conditioning to remove impurities in a gas-fired cogeneration engine is the most common technology for valorisation in medium and large size wastewater treatment plants [23], with the possibility of injecting the surplus into the natural gas grid after upgrading to remove carbon dioxide [24]. The anaerobic digestion of the sewage sludge is usually performed in large airtight cylindrical tanks (30 m in diameter and 10 m high) called digesters, within which several conditions must be met so that the bed in which the microorganisms are located is found in an ideal anaerobic environment [25]. Therefore, optimal biogas production is achieved [26]. One of these conditions is the temperature, which can be set in three different ranges: psychrophilic (ambient), mesophilic (around 37 °C) and thermophilic (around 55 °C) [13]. Operation in the last range ensures higher efficiency in the destruction of pathogens, growth rates of microorganisms and reactivity, but a higher sensitivity to specific inhibitors such as ammonia, has also been observed [27]. For these reasons, the mesophilic range (37 °C) is usually the chosen operation range [13]. Therefore, a series of conditions must be met when operating with the rector, such as thermal needs to maintain the temperature and electrical requirements for the proper working of the machinery of the digester [28]. Although anaerobic digestion is an exothermic process, the large boundary area of the digester can cause high heat release rates, so a heating demand should be met to maintain the optimal operating conditions in terms of temperature [29].

To analyse the proper integration of the biomethane produced from the WWTP into the DHCN, the assessment of the thermal demand of the district should be carried out. This can be obtained from global models based on climate data [30] or by combining dynamic simulations of buildings with GIS information [31]. Even a time expansion method can be applied to demand expressions given in current national regulations [32].

In a previous study [33], it has been demonstrated that the biomethane production of a WWTP is not enough to meet the DHCN thermal demand of the municipality whose wastewater is treated in the corresponding plant by means of a cogeneration system. This paper analyses two ways to reduce the gap between thermal demand and fuel production. On the one hand, to reduce the thermal demand of a given population, a new district is assumed to be built with the highest available standards, being the domestic hot water preparation supplied by in-situ renewable energies (solar thermal or solar PV with air source heat pumps) and with underfloor heating and cooling as final thermal installation. On the other hand, a ground source heat pump (GSHP) driven by the power produced by the cogeneration engine enhances the thermal production supplied to the DHCN. This latter measure is focused on increasing the efficiency of the fuel conversion system to meet as much as possible the thermal demand of the DHCN. The analysis is carried out in every province of Spain, obtaining both the thermal demand (heating and cooling) coverage percentage (*TDCP*) and the levelized cost of the thermal energy produced (*LCOHC*).

2. Methodology

2.1. System description

To estimate biomethane production based on equivalent inhabitants, data collection of different WWTPs in Spain has been used [34]. Biogas is produced from the decomposition of organic matter in anaerobic conditions and mainly consists of methane and carbon dioxide, with a low concentration of other gases (being especially important for corrosion issues hydrogen sulphide). Methane in biogas produced in Spain

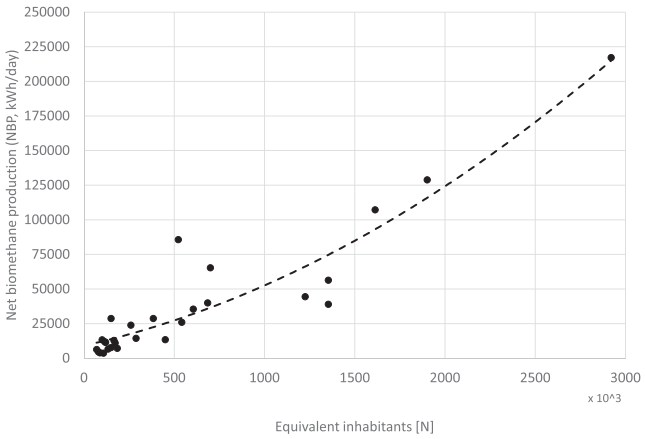

Fig. 1. Data and regression obtained for net biomethane production from WWTPs considered [34].

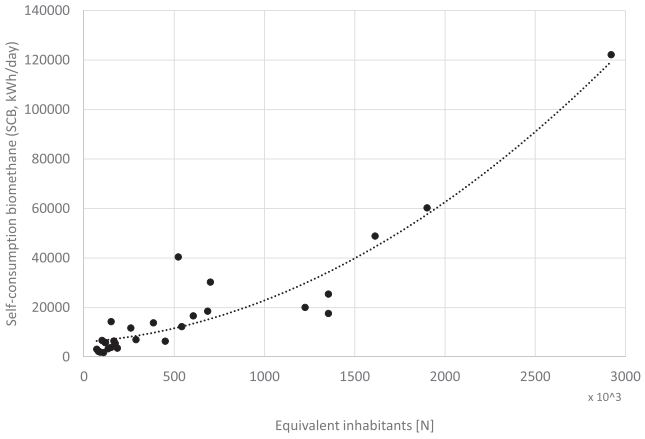

Fig. 2. Data and regression obtained for self-consumption biomethane from WWTPs considered [34].

usually ranges from 55 % to 75 % in volume [13], so 65 % has been assumed in this work. For the concentration of other gases except for carbon dioxide, a total of 5 % has been taken, thus resulting in 30 % for carbon dioxide. As both carbon dioxide and impurities will be removed to allow the injection of generated gas into the natural gas grid, the critical figure is methane composition. In addition, energy data have been taken as lower heating value (LHV) based, which in the case of CH_4 is 9.94 kWh_{th}/Nm^3 [35]. To maintain optimal conditions in the digester, a part of the gross biomethane production is self-consumed, resulting in a net biomethane production (*NBP*) and a self-consumption of biomethane (*SCB*) [13]. Fig. 1 shows the point cloud and regression obtained from the WWTP data for the *NBP*, whereas Fig. 2 for *SCB*, both in terms of equivalent inhabitants (*N*). Resulting regression curves are given in Eqs. (1) and (2), respectively.

$$NBP = 1{\cdot}10^{-8}{\cdot}N^2 + 0.0297{\cdot}N + 9,243 \ \left(R^2 = 0.88\right) \quad (1)$$

$$SCB = 4{\cdot}10^{-9}{\cdot}N^2 + 0.0119{\cdot}N + 5,032.2 \ \left(R^2 = 0.89\right) \quad (2)$$

The proposed system includes a biomethane-fired cogeneration reciprocating engine (RE) whose power feeds an electrically-driven ground source heat pump. Electrical (η_e) and thermal (η_V) efficiencies of the reciprocating engine have been taken as 37 % and 43.8 %, respectively [36]. An inverter drives the heat pump to enhance its performance at partial load. It works with R-290 and heats the water from the DHCN in winter from 35 °C to 45 °C and cools it down in summer from 24 °C to 19 °C, suitable ranges for underfloor heating and cooling

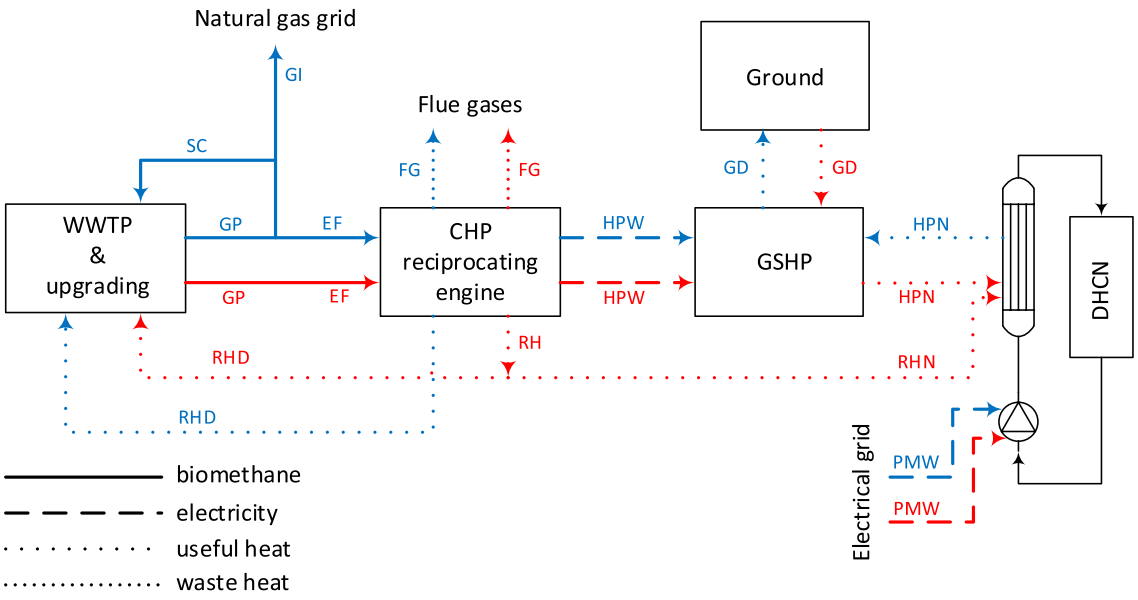

Fig. 3. Conceptual diagram at the design point of the proposed plant in any climatic zone except for α3 (50,000 equivalent inhabitants' municipality). Red colour stands for winter and blue for summer. (For interpretation of the references to colour in this figure legend, the reader is referred to the web version of this article.)

Table 1
Energy balance at each component for Fig. 3.

			Component		DHCN	
			Winter	Summer	Winter	Summer
BIOMETHANE	Gross production [GP, kW_{th}]		683	683		
	Self-consumption [SC, kW_{th}]			117		
	Grid injection [GI, kW_{th}]			297		
	Engine fuelling [EF, kW_{th}]		683	269		
ENGINE	Engine fuelling [EF, kW_{th}]		683	269		
	Recovered heat [RH, kW_{th}]	DHCN [RHN, kW_{th}]	64		64	
		Digester [RHD, kW_{th}]	235	118		
	Power [HPW, kW_e]		253	100		
	Flue gases [FG, kW_{th}]		86	51		
HEAT PUMP	Power [HPW, kW_e]		253	100		
	Ground [GD, kW_{th}]		898	998		
	DHCN [HPN, kW_{th}]		1151	898	1151	898
PUMPING	Power [PMW, kW_e]		87	64	87	64
Overall met demand [kW_{th}]					1302	834

as final air-conditioned system. In winter, the water comes from the ground at 15 °C and leaves the heat pump at 10 °C; in summer the water comes from the ground at 25 °C and exits the heat pump at 30 °C. The minimum approach temperature in both evaporator and condenser is 5 °C. These conditions lead to a COP of 4.55 and EER of 8.98. Barrella *et al.* [37] give a model of an air source water heat pump, including the operation of the heat exchangers and the compressor. This model has been adapted to the ground source heat pump, considering that water temperatures in both the condenser and the evaporator remain constant due to the temperature stability of the ground and the suitable controls implemented in the heat pump.

The heat exchangers of the heat pump always work in the same way, that is, the condenser unit releases heat to the DHCN in winter and to the ground in summer and the evaporator unit takes heat from the ground in winter and from the DHCN in summer. So, the selection of the season implies switching the external water loops (ground and DHCN) between the condenser and the evaporator with a set of valves. Due to the difference in performance between winter and summer, the design of the condenser and the evaporator has been sized for winter to maintain a similar duty in both seasons. This avoids the oversizing of the boreholes in the water loop, that exchange the heat with the ground. This design criterion requires the partial load operation in summer (even at the design point), thus exporting biomethane to the natural gas grid. The climate of the Canary Islands is clearly different from the Iberian

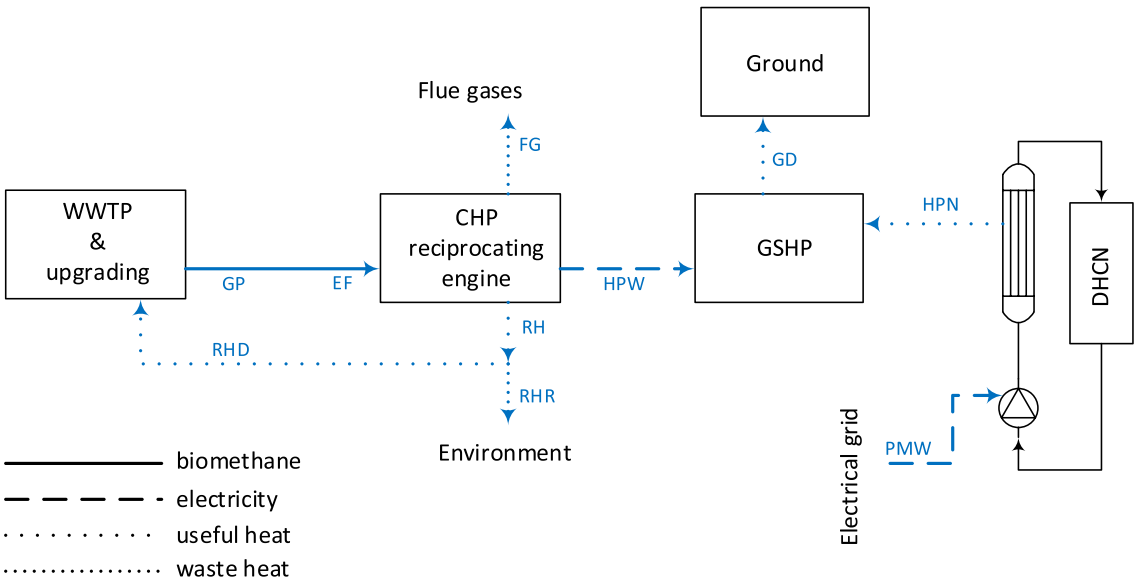

Fig. 4. Conceptual diagram at the design point of the proposed plant in the α3 zone (50,000 equivalent inhabitants). Blue colour stands for summer demand). (For interpretation of the references to colour in this figure legend, the reader is referred to the web version of this article.)

Table 2
Energy balance at each component for Fig. 4.

			Component Summer	DHCN Summer
BIOMETHANE	Gross production [GP, kW_{th}]		683	
	Engine fuelling [EF, kW_{th}]		683	
ENGINE	Engine fuelling [EF, kW_{th}]		683	
	Recovered heat [RH, kW_{th}]	Released [RHR, kW_{th}]	64	
		Digester [RHD, kW_{th}]	235	
	Power [HPW, kW_e]		253	
	Flue gases [FG, kW_{th}]		86	
HEAT PUMP	Power [HPW, kW_e]		253	
	Ground [GD, kW_{th}]		2525	
	DHCN [HPN, kW_{th}]		2272	2272
PUMPING	Power [PMW, kW_e]		162	162
Overall met demand [kW_{th}]				2110

mainland, Balearic Islands, Ceuta, and Melilla, lacking winter demand. This specific climate zone is referred in regulations as α3. As there is no winter demand in this region, the heat pump sizing is carried out with summer data, operating the heat pump and the cogeneration engine at full load in the design point, thus enhancing the cooling effect. In any zone, when partial load is required due to a low demand at DHCN, the biomethane production surplus is injected into the natural gas grid.

Fig. 3 shows the energy flows for a 50,000 equivalent inhabitants' municipality at the design point for any climate zone except for α3, Table 1 giving the detailed energy balance at each component. In winter, the gross biomethane production (683 kW_{th}) is supplied to the cogeneration (CHP) reciprocating engine, which converts it into power (253 kW_e) to drive the heat pump and recovered heat to meet the self-consumption of the digester (235 kW_{th}) and part of the DHCN demand (64 kW_{th}). The heat pump supplies 1151 kW_{th} to the DHCN and takes 898 kW_{th} from the ground. In summer, the operation is similar except for the working of both the heat pump and cogeneration engine at partial load. In this case, the self-consumption of the digester is met by the recovered heat from the cogeneration engine (118 kW_{th}) and part (117 kW_{th}) of the gross biomethane production (the engine is working at partial load, so it does not produce enough recovered heat), generating a surplus which is evacuated to the natural gas grid (297 kW_{th}). This evacuation demands the upgrading process to achieve the required specifications for injection in the natural gas grid.

Fig. 4 shows the energy flows for a 50,000 equivalent inhabitants' municipality at the design point for the α3 zone, Table 2 giving the detailed energy balance at each component. In this case, the entire biomethane production is taken (683 kW_{th}) and converted into a cooling effect (2272 kW_{th}). The self-consumption (235 kW_{th}) is obtained from the recovered heat of the engine, releasing 64 kW_{th} from recovered heat not used to the environment. In this zone, no biomethane injection into the natural gas grid is produced at the design point.

Self-consumption of the digester has been taken from design conditions in winter, assuming that it is constant all year. Despite the large heat transfer area of the digester, when high ambient temperatures are reached in summer, the need to heat the digester is reduced [29], so in summer and in warm winter days the self-consumption of the digester results overestimated. In such cases, part of the recovered heat from the engine is released into the environment using an aerothermal heat exchanger, as in any conventional cogeneration installation.

Eqs. (3) and (4) give the heating ($\dot{Q}_{HA}$) and cooling ($\dot{Q}_{CA}$) thermal power available to meet the DHCN demand at the design point. The former (Eq. (3)) is obtained from the conversion of the gross biomethane production into electricity which drives the heat pump and heat recovered from the engine, once the self-consumption of biomethane is retired. That is, the self-consumption of biomethane in winter is taken from the recovered heat of the engine, remaining the rest available for the DHCN. The latter (Eq. (4)) is obtained in a similar way, but with two differences. On the one hand, note that *EER* (8.98) is used in α3 zone whereas *COP-1* (3.55) is used elsewhere. This is due to the fact that in α3 zone the GSHP has been designed for summer (as a sole season), while in the other zones the design has been done for winter. Thus, the heat taken from the DCHN heat exchanger in the evaporator is equal to the heat taken from the ground in winter. On the other hand, Figs. 3 and 4 show that *SCB* in summer is meet with the recovered heat from the engine, releasing part of it into the environment in α3 zone or supported by part of the surplus of biomethane elsewhere. The heat released by the GSHP

in both cases is sent to the ground.

Both available thermal power values are compared at each hour with the actual thermal demand ($\dot{D}_j$) explained later in order to determine the heat exchanged ($\dot{Q}_{DHCN}$) with the DHCN (Eq. (5)). In this equation the pumping thermal effect (enthalpy gain by the water due to the power consumed by the pump) over the DHCN has been included separately from the thermal power available, assigned to the system cogeneration engine/heat pump. Finally, Eqs. (6) and (7) give the biomethane consumption of the engine in winter ($\dot{F}_W$) and summer ($\dot{F}_S$). Eq. (6) considers that recovered heat from the engine is always supplied to the digester in order to meet the self-consumption of biomethane. At high thermal demands (engine at high load) the recovered heat from the engine ($\dot{F}_W \bullet \eta_V$) exceeds the demand of the digester, supplying the surplus to the DHCN; otherwise, part of the biomethane not consumed by the engine is provided to the digester. In summer (Eq. (7)) the cooling demand is removed by the evaporator of the GSHP.

According to Eq. (5), sometimes, the heating or cooling available from the system might exceed the demand. In such cases, the engine and the heat pump modulate their capacity, so the biomethane not consumed is injected into the natural gas grid.

$$\dot{Q}_{HA} = \begin{cases} 0 & only\ in\ \alpha 3\ zone \\ \underbrace{\left(\frac{NBP+SCB}{24}\right)\cdot\eta_e\cdot COP}_{heat\ from\ GSHP} + \underbrace{\left(\frac{NBP+SCB}{24}\right)\cdot\eta_V - \left(\frac{SCB}{24}\right)}_{net\ heat\ recovered\ from\ engine} & otherwise \end{cases} \tag{3}$$

$$\dot{Q}_{CA} = \begin{cases} \left(\frac{NBP+SCB}{24}\right)\cdot\eta_e\cdot EER & only\ \ in\ \ \alpha 3\ \ zone \\ \left(\frac{NBP+SCB}{24}\right)\cdot\eta_e\cdot(COP-1) & otherwise \end{cases} \tag{4}$$

$$\dot{Q}_{DHCN} = \begin{cases} min\left\{\dot{D}_j; \dot{Q}_{HA} + \dot{W}_p\right\} & in\ winter \\ min\left\{\dot{D}_j; \dot{Q}_{CA} - \dot{W}_p\right\} & in\ summer \end{cases} \tag{5}$$

$$\dot{F}_W = \begin{cases} \dfrac{\dot{Q}_{DHCN} - \dot{W}_p + \dfrac{SCB}{24}}{COP\cdot\eta_e + \eta_V} & if\ \ \dfrac{\dot{Q}_{DHCN} - \dot{W}_p + \dfrac{SCB}{24}}{COP\cdot\eta_e + \eta_V} > \dfrac{SCB}{24\cdot\eta_V} \\ \dfrac{\dot{Q}_{DHCN} - \dot{W}_p}{COP\cdot\eta_e} & otherwise \end{cases} \tag{6}$$

$$\dot{Q}_{CA} = \begin{cases} \underbrace{\left(\frac{NBP+SCB}{24}\right)\cdot\eta_e\cdot(EER+1)}_{Ground} - \underbrace{\left(\frac{NBP+SCB}{24}\right)\cdot\eta_e}_{Power} & only\ \ in\ \ \alpha 3\ zone \\ \left(\frac{NBP+SCB}{24}\right)\cdot\eta_e\cdot(COP-1)\cdot\left(\underbrace{1+\frac{1}{EER}}_{Ground} - \underbrace{\frac{1}{EER}}_{\sim\ Power}\right) & otherwise \end{cases} \tag{9}$$

$$\dot{F}_S = \frac{\dot{Q}_{DHCN} + \dot{W}_p}{EER \bullet \eta_e} \tag{7}$$

To understand the contribution of each source of the engine/heat pump system to the heating and cooling effect at design point, Eqs. (3) and (4) can be rewritten as Eqs. (8) and (9). Eq. (8) shows three sources contributing to the heating effect: ground with the thermal energy taken in the evaporator of the GSHP, power from the engine supplied to the GSHP in the compressor and part of the recovered heat from the engine, once the self-consumption of biomethane has been removed. Eq. (9) shows the net contribution of the ground to the cooling effect, performing as a sink for both the thermal energy taken in the evaporator and the power consumed by the compressor of the GSHP. Regarding the power consumption by the pumping system, it behaves as a heat source in winter (adding to the heating thermal power available) and as a thermal load in summer (adding to the cooling demand from the DHCN).

$$\dot{Q}_{HA} = \underbrace{\left(\frac{NBP+SCB}{24}\right)\cdot\eta_e\cdot(COP-1)}_{Ground} + \underbrace{\left(\frac{NBP+SCB}{24}\right)\cdot\eta_e}_{Power} + \underbrace{\left(\frac{NBP+SCB}{24}\right)\cdot\eta_V - \left(\frac{SCB}{24}\right)}_{Recovered\ \ heat} \tag{8}$$

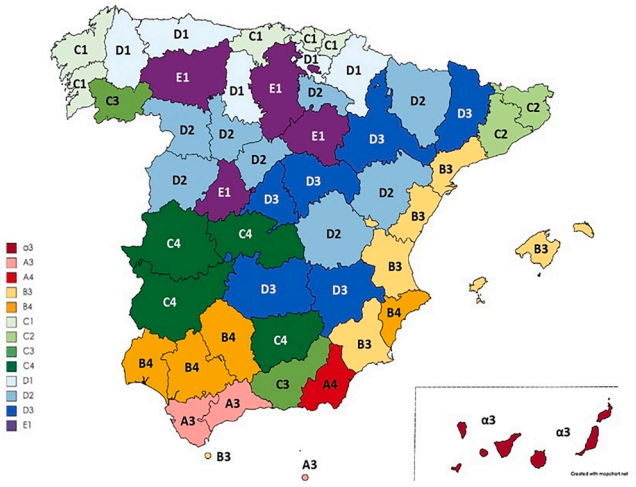

Fig. 5. Climate zones in Spain (the rating of each province has been assigned according to the value of its capital city).

2.2. Thermal energy demand

Between the different techniques to assess the heating and cooling demand of a dwelling, a time expansion method over expressions available at current Spanish regulations has been developed [32]. This procedure does not require local details about the dwelling, such as

Table 3
Coefficients required to obtain the reference specific thermal demand [38].

	Winter		Summer	
	α [kWh_{th}/m^2]	β [kWh_{th}/m^2]	α [kWh_{th}/m^2]	β [kWh_{th}/m^2]
Single-family house	9.29	54.98	−4.24	20.41
Block dwellings	3.51	39.57	−3.44	14.44

Table 4
Calculation of RAD and DD in Eq. (4) [40]. Summations are extended over all the hours of each season, taking 90 days in winter and 122 in summer.

	Winter	Summer
RAD	$\frac{\sum_{k=1}^{24\bullet 90} r_k}{3}$	$\frac{\sum_{k=1}^{24\bullet 122} r_k}{4}$
DD	$\frac{\sum_{k=1}^{24\bullet 90} \Delta T_k}{24 \bullet 3}$	$\frac{\sum_{k=1}^{24\bullet 122} \Delta T_k}{24 \bullet 4}$
ΔT_k	$\begin{cases} T_b - T_k & if T_b > T_k \\ 0 & otherwise \end{cases}$	$\begin{cases} T_k - T_b & if T_k > T_b \\ 0 & otherwise \end{cases}$

orientation, windows surface, and inner distribution, but uses the location, dwelling surface, and an insulation indicator designed as an energy performance index (*EPI*) [38]. Thus, the thermal demand assessment of the DHCN can be carried out globally, without the need of using individual dwelling features.

The procedure to assess the energy demand in Spain, both in winter (October to May) and in summer (June to September), as a function of the climate severity index (*CSI*) is established in the Building Technical Code (BTC) [38]. The climate severity index is a dimensionless indicator of how harsh the climate is, establishing five tiers for winter (A to E, being A the warmest winter) and four for summer (1 to 4, meaning 1 the lack of summer demand). Thus, each location in Spain is assigned a code of two characters (A to E plus 1 to 4), indicating the climate zone. For instance, a zone with a continental climate like Madrid is identified with the D3 code. Fig. 5 shows Spain's different climatic zones (values have been assigned using the case of the capital of each province). The procedure to assess the energy demand is similar for both seasons, so equations will be shown in a generic form, where coefficient and variables will take specific values for each season. The reference specific demand (*RD*) is the average seasonal thermal demand per unit of area of a representative cluster of buildings (a set of typologies have been simulated in the BTC to obtain a regression curve, given in Eq. (10)). Coefficients for this regression are given in Table 3 for each season and building type (thermal demand is strongly dependent on the layout of the dwelling, showing block dwellings an additional level of insulation due to the reduction of exposure to the environment). The climate severity index depends on the average accumulated global radiation over horizontal surface (*RAD*) and the degree-days (*DD*) with a base temperature (T_b) of 20 °C, according to Eq. (11). Eq. (11) is given at BTC for a short winter (December to February), whereas full winter (October to May) is required. This issue will be addressed later with a correction coefficient. The calculation of *RAD* requires the global hourly radiation over the horizontal surface (r_k), whereas the calculation of *DD* requires the hourly temperature difference (ΔT_k). Hourly values of T_k are available for each climatic zone on the web site of the BTC [39]. The calculation procedure of those two variables (*RAD* and *DD*), together with T_k values, is shown in Table 4 [40], and coefficients for Eq. (11) are provided in Table 5.

$$RD = \alpha + \beta \cdot CSI \tag{10}$$

$$CSI = aRAD + bDD + c \cdot RAD \cdot DD + d \cdot RAD^2 + e \cdot DD^2 + f \tag{11}$$

Reference specific demand and climate severity index given in Eqs. (10) and (11) are defined for the overall season (short winter, from December to February, and summer). To obtain an hourly expression of the specific reference demand, a Taylor series expansion of first order around (*RAD*, *DD*) over *CSI* has been proposed [37]. In this expansion, all the hours of the year are considered, so expanding the winter season from October to May. Applying this procedure to Eq. (11), the seasonal *RD* given in Eq. (10) is converted into hourly specific reference demand in Eq. (12), where the "*j*" index is extended to all the hours from October to May (1 to 5832) in winter and from June to September (1 to 2928) in summer. Eq. (12) requires the number of days (N_d, 243 in winter and 122 in summer) and months (N_m, 8 in winter and 4 in summer) in the season. Auxiliary coefficients (ρ and βδ) have been defined for convenience in Eqs. (13) and (14), respectively. The star in the hourly specific reference demand means that a correction is needed to consider two different issues, firstly the effect of the radiation (explained later) and secondly, the fact that five additional months have been included with respect to the original correlation in winter.

The radiation correction is performed because, at some hours, its value is high enough to result in a negative demand. When this occurs, the thermal demand at that hour is set to zero. Parallel to this, to consider the inclusion of additional months in the formulation, a reduction coefficient (C_r) is defined as the ratio of the actual specific seasonal demand (RD^a), (an updated value of *RD* given in regulations [41]) to the summation of $\dot{RD}_j^*$ over the overall hours (*oh*) of each season (5832 in winter and 2928 in summer). Thus, the resulting corrected hourly specific reference demand $\left(\dot{RD}_j\right)$ is given in Eq. (15). Note that $\dot{RD}_j^*$ and $\dot{RD}_j$ stands for specific thermal energy demand per hour, so they can be understood as an average thermal power demand (kWh_{th}/h) in that hour.

$$\dot{RD}_j^* = \frac{\alpha + \beta \bullet (WSI - \rho \bullet RAD - \delta \bullet DD)}{24 \bullet N_d} + \left(\frac{\beta \bullet \rho}{N_m}\right) \bullet r_j + \left(\frac{\beta \bullet \delta}{24 \bullet N_m}\right) \bullet \Delta T_j \tag{12}$$

Table 6
Values for ~~R~~ R_S in Eq. (9) [38].

		Single-family house	Block dwellings
Winter	α	–	–
	A	1.7	1.7
	B	1.6	1.7
	C	1.5	1.7
	D	1.5	1.7
	E	1.4	1.7
Summer	1	–	–
	2	1.5	1.6
	3	1.4	1.5
	4	1.4	1.5

Table 5
Coefficients required to obtain the climate severity index (*CSI*) [40].

	a [m^2/kW_{th}]	*b* [1/K]	*c* [$m^2/(kW_{th} \cdot K)$]	*d* [$m^4/(kW_{th})^2$]	*e* [$1/K^2$]	*f* [p.u.]
Winter	$-8.35 \cdot 10^{-3}$	$3.72 \cdot 10^{-3}$	$-8.62 \cdot 10^{-6}$	$4.88 \cdot 10^{-5}$	$7.15 \cdot 10^{-7}$	$-6.81 \cdot 10^{-2}$
Summer	$3.724 \cdot 10^{-3}$	$1.409 \cdot 10^{-2}$	$-1.869 \cdot 10^{-5}$	$-2.053 \cdot 10^{-6}$	$-1.389 \cdot 10^{-5}$	$-5.434 \cdot 10^{-1}$

$$\rho = a + 2 \cdot d \cdot RAD + c \cdot DD \tag{13}$$

$$\delta = b + c \cdot RAD + 2 \cdot e \cdot DD \tag{14}$$

$$\dot{RD}_j = \underbrace{\dot{RD}_j^* \cdot \left(\frac{RD^a}{\sum_{j=1}^{oh} \dot{RD}_j^*} \right)}_{C_r} \cdot \begin{cases} 1 & if\ \dot{RD}_j^* > 0 \\ 0 & otherwise \end{cases} \tag{15}$$

The specific reference demand is given at BTC for an average reference building cluster, so the hourly specific reference demand given at Eq. (15) should be corrected to consider the actual insulation level employed and the variety of typologies in the building database. Two parameters are used to calculate this correction. On the one hand, the *EPI* considers the insulation level; on the other hand, the variation of the demand according to the building database is considered with the ratio of *RD* (an average value of the whole stock of the building database) to the reference specific demand of the 10-th percentile of this stock. Such ratio (R_s) is given in Table 6 [38]. This correction calculates the hourly absolute demand ($\dot{D}_j$), from Eq. (16), where the conditioned area (A) is included. The average conditioned area per habitant in Spain has been calculated from data collected in [42], resulting in 38.02 m^2. Concerning the *EPI* values, they have been set to 0.075, according to a high insulation level (A score). This assumption is one of the two solutions set out in this paper to reduce the gap between the biomethane production and the thermal demand from the district. Such a level is far from the current situation in Spain, but it is aligned with the future expectations. The BTC is being updated at least every five years to consider the current state of the art in efficiency and insulation.

$$\dot{D}_j = A \bullet \dot{RD}_j \bullet \left(\frac{1 + (EPI - 0.6) \bullet 2 \bullet (R_S - 1)}{R_S} \right) \tag{16}$$

Eq. (17) gives the thermal demand coverage percentage (*TDCP*) as a ratio between met thermal demand (*MD,* Eq. (18)) and DHCN demand (*ND,* Eq. (19)).

$$TDCP = \left[\frac{MD}{ND} \right] \bullet 100 \tag{17}$$

$$MD = \sum_{1}^{8760} \dot{Q}_{DHCN} \tag{18}$$

$$ND = \sum_{1}^{8760} \dot{D}_j \tag{19}$$

2.3. Economic model

To avoid going into the economic details of the WWTP, the biomethane production cost from this kind of plants has been considered (35 €/MWh_{th} biogas price plus 50 €/MWh_{th} upgrading costs [13]), being sold the thermal production to the DHCN. Income from the injection of biomethane surpluses (design point in summer and whenever is required) has not been considered. The investment cost only includes the thermal energy generation station (heat pump and reciprocating engine, with all the auxiliary equipment required). Thus, the investment cost of the DHCN is not included in the cost of the thermal energy, assuming that it is a municipal infrastructure. That is, the investment cost of the network is covered by the city council, which will recover it from taxes, such as municipal solid waste collection and treatment, road maintenance and so on. Similarly, the investment for the final air-conditioning installation (underfloor heating and cooling) is not considered, as it will be covered by the consumer within the cost of the dwelling. To consider the overall cost of the thermal energy produced, the levelized cost of heating and cooling (*LCOHC*) is considered, based on the formulation of Bejan [43]. The levelization process includes the overall costs of the system during its lifespan (N_y) discounting and accumulating them to the present, and then amortizing them along the duration of the project. The amortization is carried out using the capital recovery factor (*CRF*), defined in Eq. (20) using the weighted average capital cost (*wacc*) and N_y. Constant escalation levelization factor (*CELF*) defined in Eq. (21) projects to the future the present costs using the nominal escalation rate (r_n) and then discounts them to the present time using *wacc*, to finally accumulate all the discounted costs. Levelized cost (Eq. (22)) includes the investment (both in heat pump, INV_{HP}, and in reciprocating engine, INV_{RE}), costs of biomethane (from the costs at zero year C_0^F), costs for powering the pumps of the DHCN (from the costs at zero year C_0^P) and costs of maintenance (from the costs at zero year C_0^M), all of them referred to *MD*.

Table 7
Coefficients for investments (Eqs. (23) and (24)) and maintenance cost (Eq. (25)) [36,44].

Heat pump	HP_0 [€]	102,940
	HP_1 [kW_{th}]	132.2
Reciprocating engine	RE_0 [€]	106,673
	RE_1 [€/kW_e]	1258
Maintenance	M_0 [€/($MWh_e \bullet kW_e^{0.199}$)]	59.394

Table 8
Economic parameters considered.

Parameter	Value
Weighted average capital cost, *wacc* [p.u]	0.075
Nominal escalation rate, r_n [p.u.]	0.025
Life span, *Ny* [years]	15

$$CRF = \frac{wacc \bullet (1 + wacc)^{Ny}}{(1 + wacc)^{Ny} - 1} \tag{20}$$

$$CELF = \left[\frac{\left(\frac{1+r}{1+wacc}\right) \bullet \left(1 - \left(\frac{1+r}{1+wacc}\right)^{Ny}\right)}{1 - \left(\frac{1+r}{1+wacc}\right)} \right] \bullet CRF \tag{21}$$

$$LCOHC = \frac{(INV_{HP} + INV_{RE}) \bullet CRF + C_0^F \bullet CELF + C_0^P \bullet CELF + C_0^M \bullet CELF}{MD} \tag{22}$$

The investment for the heat pump has been determined as a scale law (Eq. (23)) from a project given in [44], whereas a regression curve taken from [36] has been used for the investment for the reciprocating engine (Eq. (24)). In both cases, the investment includes both the main equipment (GSHP or RE) and the auxiliary components (boreholes at GSHP and dissipation and recovery heat exchangers at RE). Power consumption in pumps has been estimated as 1/14 of the thermal energy met [45], with an electrical tariff of 75.19 €/MWh_e [46]. Maintenance costs are given in Eq. (25), where the regression given in brackets has been derived from [36] to assess the maintenance cost for the engine. In this equation, E stands for the electrical energy produced by the engine per year, and the factor 1.1 considers the maintenance cost of the heat pump (10 % of the maintenance cost for reciprocating engine). Table 7 gives the coefficients for Eqs. (23) to (25), and Table 8 shows the economic parameters used to calculate the levelized costs.

$$INV_{HP} = HP_0 \bullet \left(\frac{\dot{Q}_{con}}{HP_1} \right)^{0.6} \tag{23}$$

$$INV_{RE} = RE_0 + RE_1 \bullet \dot{W} \tag{24}$$

Table 9
Contributions of energy sources/sinks to heating and cooling DHCN for 50,000 equivalent inhabitants' municipality at the design point. Positive values stand for energy flows towards the network.

	Biomethane		Met Demand			
	Gross biomethane production [kW]	Biomethane injection into the natural gas grid [kW]	Ground [kW]	Engine power [kW]	Engine Recovered heat [kW]	Pumping power [kW]
Winter	683	0	898	253	64	87
Summer (all zones except for α3)	683	−297	−998	100	0	64
Summer (only α3)	683	0	−2525	253	0	162

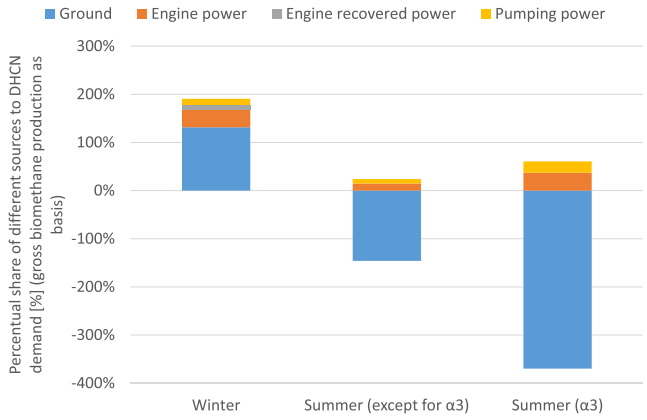

Fig. 6. Contribution of each source to the heating or cooling demand at the design point of the system (gross biomethane production has been taken as basis).

$$C_0^M = 1.1 \bullet \left\{ M_0 \bullet \dot{W}^{-0.199} \right\} \bullet E \tag{25}$$

3. Results and discussion

The analysis has been focused in 50,000 equivalent inhabitants WWTP since this size is the most common in Spain. Table 9 shows the contributions of each thermal source/sink to the heating or cooling demand at design point, considering positive signs for energy flows towards the DHCN. These values have been plotted in Fig. 6 in percentual format, taking the gross biomethane production as basis. Regarding the global efficiency of the system, in winter each energy unit of gross biomethane production is converted into 1.78 thermal units supplied to the DHCN, which takes 0.13 units from the electrical grid to meet the consumption of pumps. In summer, 1.22 cooling units are removed from the DHCN in any climatic zone except for α3, where 3.09 are taken due to its special sizing criteria. The ground contribution is, by far, the most important between different sources/sinks. Such an important contribution should be considered in the location of the boreholes to exchange heat between the heat pump and the ground. So, although the thermal power exchanged in summer and winter is similar, winter lasts more time, so in general, more energy will be taken from the ground than it will be injected. Depending on the thermal properties of the ground, it will be able to manage this unbalance with the surrounding ground. Still, if such unbalance is not compensated, the average temperature of the ground will tend to decrease, penalizing heating performance and improving cooling one.

Table 10 shows the thermal demand of the DHCN, the system's met demand and the thermal demand coverage percentage in winter and summer in every climate zone. Annual coverage (*TDCP*, Eq. (17)) is also included in the table. Fig. 7 shows the *TDCP* at each province, represented by the climate zone of its capital. Comparing this information with Fig. 5 it can be observed that, the lower the climate severity, the higher the *TDCP*. This fact is stated in Fig. 8, which shows that the lowest *TDCP* can be reached either with extreme winter (E1), mild winter but extreme summer (A4, B4, and C4), or severe winter and summer (D3). On the other hand, the highest *TDCP* is reached with mild winters and fresh summers (C1, C2) or high-intermediate summer without winter demand (α3).

Fig. 8 can be better understood by comparing winter and summer behaviour. In this sense, Fig. 9 plots the demand given in Table 10. Although the gross biomethane production is fixed (683 kW_{th} along 8760 h per year, that is, 3983 MWh_{th} in winter and 2000 MWh_{th} in summer), it can be seen that the absolute met demand is not constant, increasing with the climate severity of each zone. So, winter met demand increases from A to E winter zones, the same as summer met demand from 1 to 4 (α3 is an exception due to its particular sizing criterion). This behaviour is explained due to the saturation effect of Eq.

Table 10
Seasonal thermal demand of the DHCN, met demand by the system and thermal demand coverage percentage at every climate zone. Annual coverage (*TDCP*) is also included.

	Winter			Summer			Annual		
Climate zone	Demand [MWh_{th}]	Met demand [MWh_{th}]	Thermal demand coverage percentage [%]	Demand [MWh_{th}]	Met demand [MWh_{th}]	Thermal demand coverage percentage [%]	Demand [MWh_{th}]	Met demand [MWh_{th}]	Thermal demand coverage percentage [%]
C1	10,442	5305	51	0	0	0	10,442	5305	51
α3	0	0	0	8979	4362	49	8979	4362	49
C2	10,442	5273	51	3125	1130	36	13,567	6402	47
A3	4094	3394	83	8979	1598	18	13,073	4993	38
B3	6200	4154	67	8979	1579	18	15,180	5733	38
D2	15,723	5622	36	3125	1085	35	18,848	6707	36
D1	15,723	5590	36	0	0	0	15,723	5590	36
C3	10,442	5281	51	8979	1611	18	19,422	6892	36
B4	6200	4151	67	12,656	2145	17	18,856	6296	33
A4	4094	3387	83	12,656	2144	17	16,749	5531	33
C4	10,442	5273	51	12,656	2128	17	23,098	7401	32
D3	15,723	5578	36	8979	1602	18	24,702	7179	29
E1	21,122	5959	28	0	0	0	21,122	5959	28

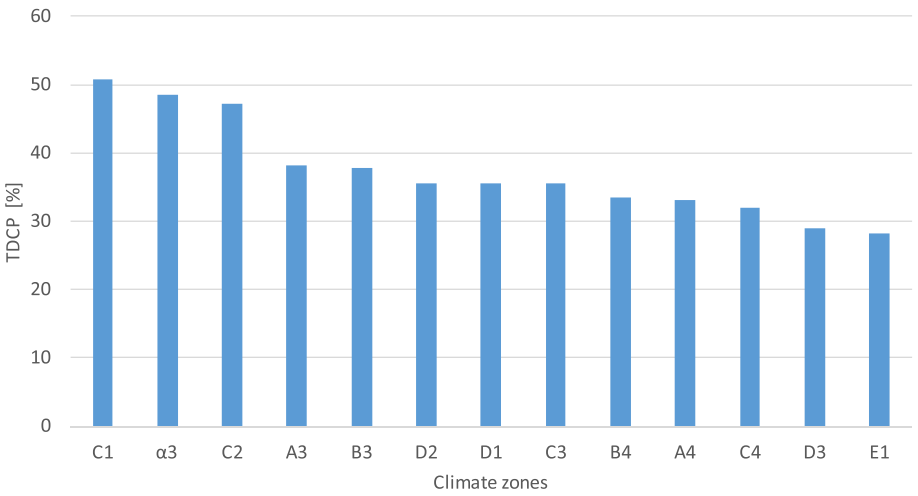

Fig. 7. TDCP in Spain (the rating of each province has been assigned according to the value of its capital).

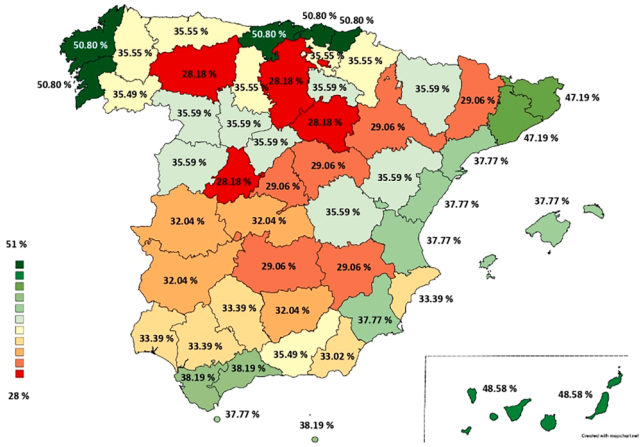

Fig. 8. TDCP in Spain according to the climate zone.

(5), that is, the system works at partial load in any location. So, the maximum thermal energy generable in winter (7090 MWh_{th}) and summer (6180 MWh_{th} in α3 and 2040 MWh_{th} otherwise) are never reached. Although the curtailment effect of the partial load is reduced when climate severity is increased, the gain in thermal demand is higher, so the seasonal coverage is reduced. Apart from α3, A and B zones have high summer severity (3 or 4), so their high winter coverage is compensated with a low summer one, moving A3, A4, B3, and B4 zones to an intermediate level of *TDCP*. However, in C and D, there are two low levels of summer severity (1 and 2), which gives C1 and C2 the highest value of *TDCP*, whereas D1 and D2 range at an intermediate level for their higher winter severity, where C3 and C4 are also included due to high summer severity are compensated with intermediate winter one. Finally, the lowest *TDCP* is reached in the E1 zone with the largest winter severity, having D3 a similar value due to high summer severity compensates the lower winter severity than in E1. Regarding the α3 zone, its *TDCP* is very high due to its special design.

Fig. 10 explores selected performance indicators (*TDCP* and *LCOHC*) as a function of the absolute network thermal demand. Fig. 10.a shows the highest coverage levels at low and balanced thermal demands (bottom left corner). In contrast, lowest levels are reached at large winter demand (top left corner) and medium winter demand with large summer one (top right quadrant). As biomethane production is fixed, low and balanced demands exhibit the highest coverage levels. However, low winter demands with high summer ones (bottom right corner) reduce their coverage due to the working at a partial load of the system in summer (except for α3, with nearly 9000 MWh_{th} of summer demand and zero winter demand). Fig. 10.b shows the lowest levelized costs at low winter demand and medium summer one, which corresponds with high *TDCP*, that is, the system produces a lot of energy. However, from

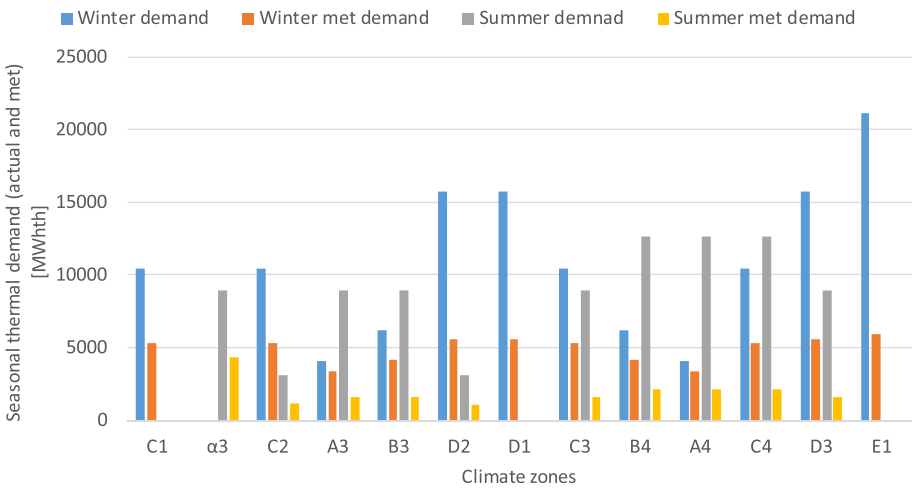

Fig. 9. Seasonal actual and met demand at every climate zone.

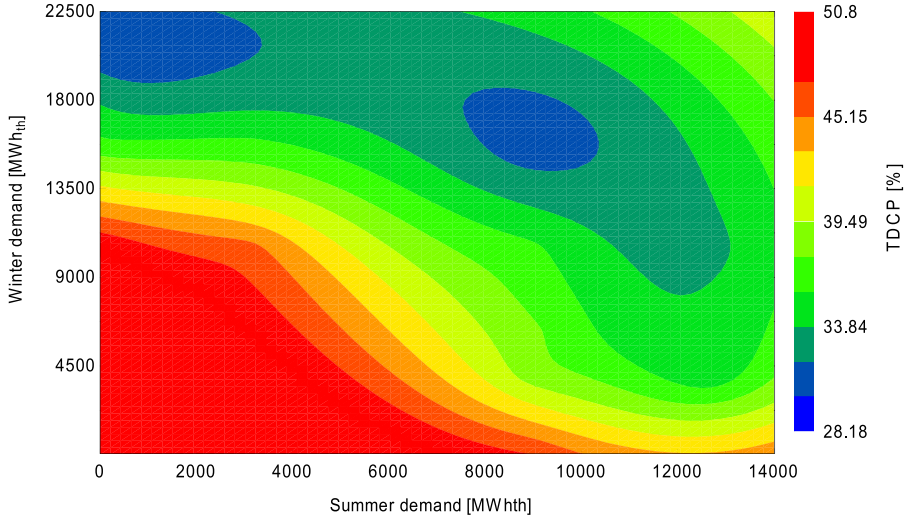

Fig. 10. TDCP (a) and LCOHC (b) as a function of absolute covered demand in winter and summer.

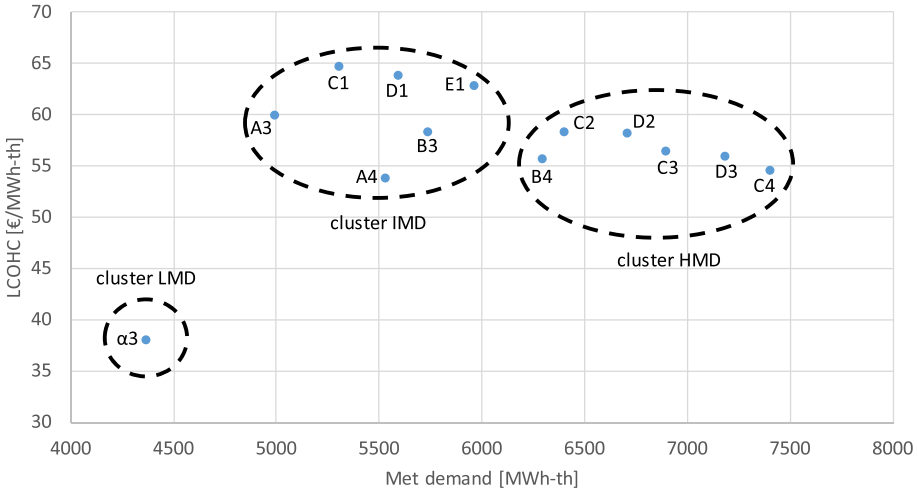

Fig. 11. Clustering of climate zones according to levelized cost of heating and cooling and overall (heating and cooling) met demand.

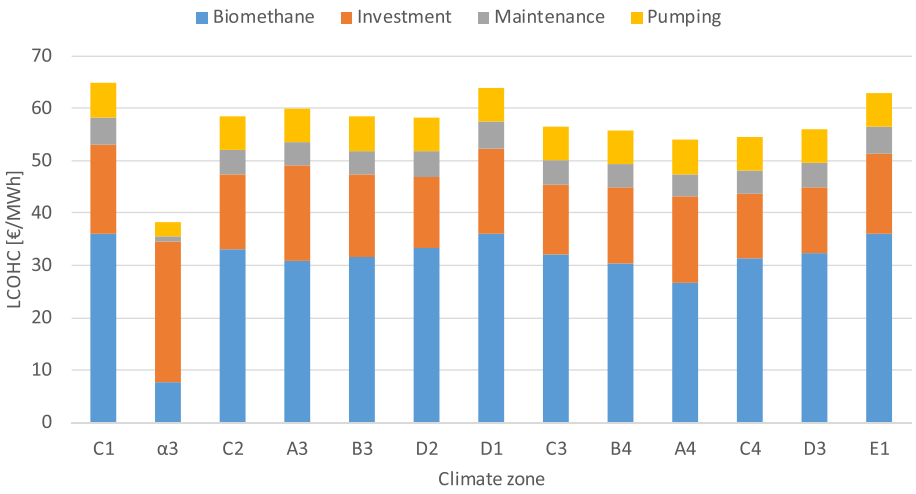

Fig. 12. Breakdown of levelized cost of heating and cooling.

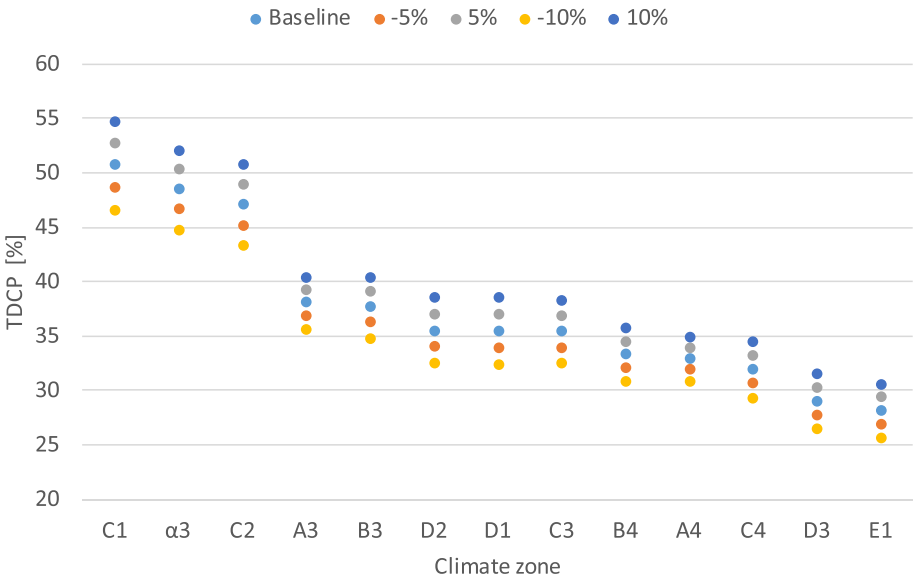

Fig. 13. Sensitivity analysis (absolute format) of thermal demand coverage percentage against a simultaneous variation (±5 % and ± 10 %) in both biomethane production and price.

medium to high winter thermal demands, the levelized cost increases at any summer demand. In fact, at low thermal demand (bottom left corner) or a high one (top right corner), the cost is maximum due to the low production or low coverage, respectively. In any case, it is noticeable that costs obtained are lower than the ones reached with current technologies (chillers and condensation boilers), even in centralised systems, which exceed 70 €/MWh$_{th}$ [37]. These aspects are summarised in Fig. 11, which shows three clusters:

- Cluster LMD, with lowest cost and lowest met demand, in Canary Islands.
- Cluster IMD, with highest cost and intermediate met demand, in coolest winters with fresh summers or warm winters with hottest winters.
- Cluster HMD, with intermediate cost and high met demand, in mild winters and summers.

Fig. 11 reveals similar levelized costs in all climatic zones except for α3. This is explained by the significant contribution of biomethane cost into the levelized cost, as can be seen in Fig. 12, where a share between 50 % and 60 % is obtained everywhere except for α3. As fuel expenditures are proportional to demand, cost, referred to demand, tends to be constant. The case of α3 is different due to the high conversion efficiency reached (3.09 kW of cooling per kW of biomethane) reduces a lot the contribution of biomethane cost, converting investment into the most crucial contribution to levelized cost. As the heat pump is more significant in this zone than in the rest of the locations, the levelized investment cost is higher than in the rest of the zones, but the reduction in biomethane cost compensates this by far. Regarding the absolute met demand, climate zones in cluster HMD combine intermediate to high winter and summer severity to reduce the curtailment of the heating and cooling capacity of the system. Finally, climate zones in cluster IMD only have one high severity season, which reduces the absolute met demand.

The two measures proposed in this work to reduce the gap between biomethane production and thermal demand from the same population have been exploited up to their limits using a very high level of insulation and a ground source heat pump instead of an air source one. Even with such a hypothesis, the average *TDCP* is about 35 %. Both assumptions are technically feasible but do not apply to existing buildings. However, the low coverage makes it possible to implement both measures in new districts built with the most exigent regulations (the EU

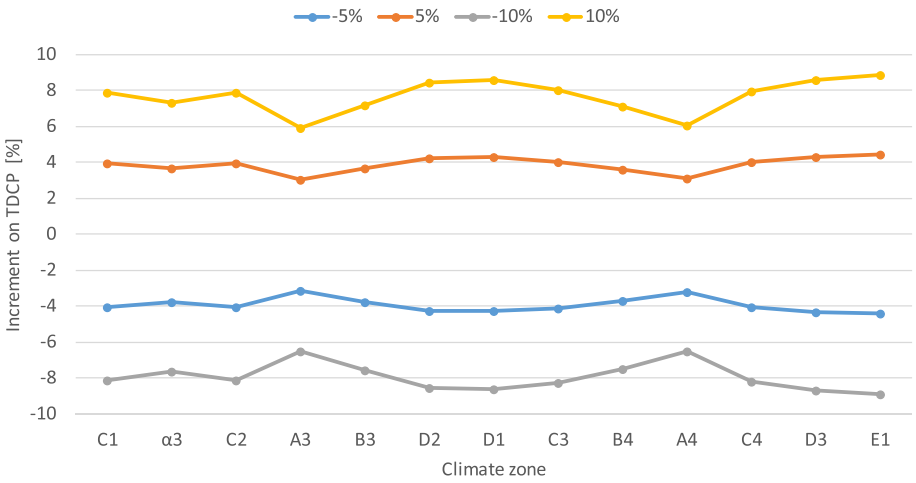

Fig. 14. Sensitivity analysis (specific format) of thermal demand coverage percentage against a simultaneous variation (±5 % and ± 10 %) in both biomethane production and price.

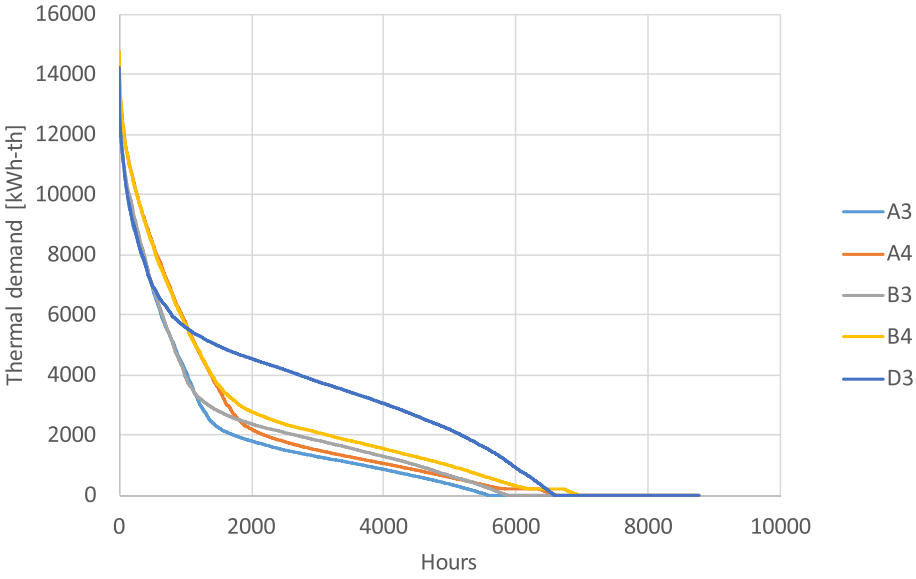

Fig. 15. Cumulative thermal demand profile of low winter severity zones with high summer severity (A3, A4, B3, and B4) compared with a high winter and summer severity zone (D3).

asks for revisions in periods lower than 5 years, according to the current state of the art). If the insulation standard was not so high, biomethane from an additional population might be considered, excluding such additional population from the DHCN. In this sense, the new district would take advantage of the wastewater of the entire population in the municipality. Social dwellings might constitute this new district due to the lower cost of thermal services. Another option would be to change or add new sources of biomethane, such as landfill gas or digestion of the organic fraction of municipal solid wastes.

A sensitivity analysis has been carried out to assess the influence of the two critical parameters of the plant: biomethane production (Eqs. (1) and (2)) and biomethane price (85 €/MWh$_{th}$, including both production and upgrading). Two scenarios have been considered in the sensitivity study in both key parameters: 5 % and 10 %. These values for biomethane production are according to R^2 in regression Eqs. (1) and (2), leading to a standard deviation round to 6 %. The biomethane prices are according to regressions given in [13].

Fig. 13 gives the sensitivity analysis for *TDCP* in an absolute format. It can be seen that the separation between each scenario is not constant along the climate zone. This is highlighted in Fig. 14, which translates Fig. 13 into a specific format. Fig. 14 reveals that A3 and A4 zones exhibit low sensitivity to biomethane production, B3 and B4 a medium sensitivity, and the rest of the zones a nearly constant sensitivity. To understand this behaviour, it is necessary to compare the cumulative thermal demand profiles of these zones, shown in Fig. 15. In zones with low winter severity (A3, A4, B3, and B4), the cross between the profile with the heating or cooling available thermal power (around 1000 kW$_{th}$) occurs in the low slope zone, generating a triangular area in the right side where the system operates at partial load. So, although biomethane production increases, the gain is moderated because the partial load zone is relevant. This is less important when winter severity increases (B zone regarding A zone). However, with high winter severity (D3), the profile cross with the heating available thermal power occurs close to the maximal operating hours, achieving a large sensitivity to the biomethane production.

Fig. 16 gives the sensitivity analysis for *LCOHC* in an absolute format. It can be observed that the separation of the new scenarios from the baseline is more regular in Fig. 16 than in 13. According to previous results, the low cost in the α3 zone is another important highlight. Again, this behaviour results from the special heat pump sizing in this zone,

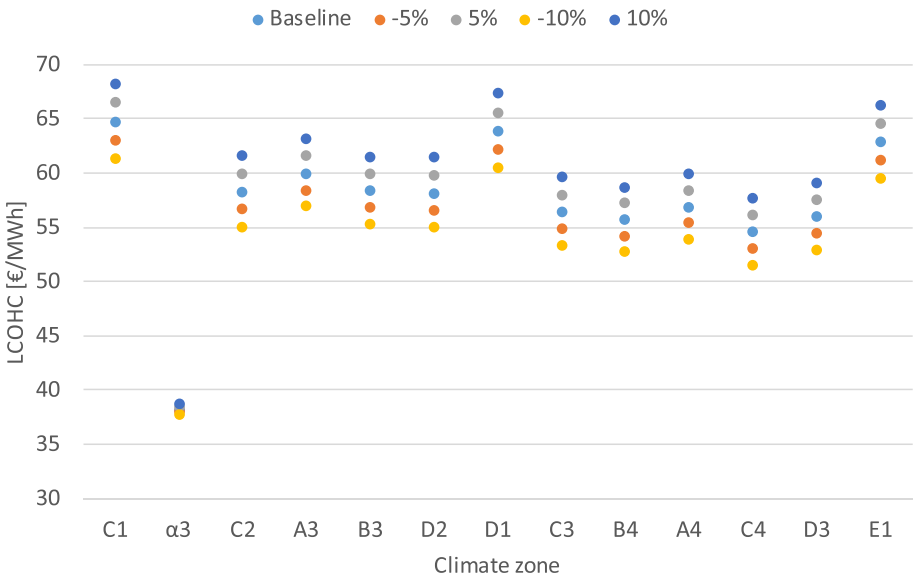

Fig. 16. Sensitivity analysis (absolute format) of levelized cost of heating and cooling against a simultaneous variation (±5 % and ± 10 %) in both biomethane production and price.

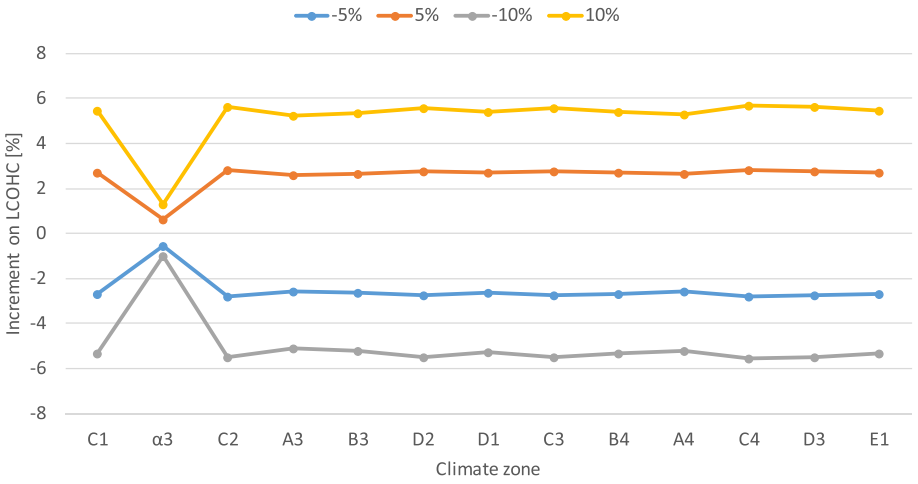

Fig. 17. Sensitivity analysis (specific format) of levelized cost of heating and cooling against a simultaneous variation (±5 % and ± 10 %) in both biomethane production and price.

achieving a high cooling amplification effect. Fig. 17 shows the sensitivity analysis in a specific format, revealing a constant variation in costs, except for α3 zone, as expected. The typical behaviour of the sensitivity of LCOHC to the analysed parameters, specially to the biomethane cost, can be explained in Fig. 12. It shows a contribution of biomethane cost to LCOHC higher than 50 % (58 % in D3 zone) in all the zones except for α3, where the heat pump has been sized for summer, thus achieving a high amplification cooling effect, which leads to a low share (20 %) of biomethane price in the *LCOHC*, being the investment component the highest contribution (70 %) in this zone. So, an increase of 5 % in biomethane price is translated into LCOHC as 2.87 % in D3 zone (and similar in other zones except for α3).

So, in summary, the sensitivity of the results against the two chosen key parameters is larger in *TDCP* (nearly proportional to gross biomethane production) than in *LCOHC*, which attenuates the variations in a factor higher than 2. The biomethane price hardly influences the α3 zone due to its heat pump's special sizing.

4. Conclusions

Methane emissions from wastewater treatment plants are usually avoided by producing biogas from the anaerobic digestion of this sludge, which also allows meeting the plant's energy needs. Once the thermal self-consumption of the digester is met, the remaining biogas can be burnt into a cogeneration unit or injected into the grid if the biogas is upgraded to biomethane. This article sets out an alternative solution for this concern, based on a ground source heat pump driven by a cogeneration reciprocating engine fuelled by the biomethane upgraded from the biogas produced in the digester. This heat pump meets the thermal demand of a district cooling and heating network owned by the municipality. As biogas is upgraded to biomethane, eventual surpluses can be injected into the natural gas grid.

Two sizing criteria have been adopted in the heat pump, one for climates with only summer demands and the other for climates with both winter and summer demands. The former seeks to maximise the cooling effect, although the location and layout of the boreholes should be carefully studied to minimise the ground average temperature increase. The latter sizes the heat pump for winter, achieving a similar

duty of heat exchangers and boreholes throughout the year. In the case of only summer demand, 3.09 units of cooling power are removed from the district heating and cooling network per unit of lower heating value of gross biomethane produced by the digester, being this conversion ratio of 1.22 in the other design. Regarding the heating mode, the ratio reaches 1.78.

Despite the high performance of the proposed system and the high insulation level assumed in the district, the percentage of met demand ranges only from 28 % to 51 %. However, levelized heating and cooling costs range between 38 and 65 €/MWhth, well below the current one with conventional technologies. Thus, it is concluded that although the system is economically feasible, the biomethane production from the sludge of the wastewater treatment plant is not enough to cover the thermal demand of the inhabitants who release the waste. Both high insulation buildings standards and the use of a district heating and cooling network owned by the municipality system requirements would be easier to comply if the thermal demand comes from a new district, where the municipality takes advantage of investment support from international infrastructure programs and the biomethane from the sludge of the entire municipality is used to fuel the proposed system. In this way, social dwellings in this district could benefit from the low costs of the system. In future works, other biomethane sources might be explored in order to increase the met demand. Such sources include landfills, the digestion of organic fraction of municipal solid wastes and wastes from central food markets.

As a concluding remark, the proposed system can meet de thermal demand of a district of a municipality (population in the district between 28 % and 51 % of the municipality, depending on the climate zone of the location) using as fuel the biomethane from the anaerobic digestion of the sludge of the wastewater treatment plant of the entire municipality.

Declaration of Competing Interest

The authors declare that they have no known competing financial interests or personal relationships that could have appeared to influence the work reported in this paper.

Data availability

Data used are available at references.

Acknowledgments

The authors acknowledge the support of the Rafael Mariño Chair in New Energy Technologies for this research.

References

[1] International Energy Agency. Directorate of Sustainable Energy Policy. Transition to sustainable buildings strategies and opportunities to 2050. Organization for Economic, 2013.
[2] J. Lizana, C. Ortiz, V.M. Soltero, R. Chacartegui, District heating systems based on low-carbon energy technologies in Mediterranean areas, Energy 120 (2017) 397–416.
[3] European Commission. A Roadmap for moving to a competitive low carbon economy in 2050. Publications Office of the European Union, 2011.
[4] N. Scarlat, J.F. Dallemand, F. Monforti-Ferrario, et al., Renewable energy policy framework and bioenergy contribution in the European Union - an overview from national renewable energy action plans and progress reports, Renew. Sustain. Energy Rev. 51 (2015) 969–985.
[5] V.M. Solterom, S. Rodríguez-Artacho, R. Velázquez, R. Chacartegui, E3S Web Conference 22 (2017) 00163.
[6] Y. Li, L. Fu, S. Zhang, Technology application of district heating system with Cogeneration based on absorption heat exchange, Energy 90 (2015) 663–670.
[7] R. Chacartegui, M. Carvalho, R. Abrahão, J. Becerra, Analysis of a CHP plant in a municipal solid waste landfill in the South of Spain, Appl. Therm. Eng. 91 (2015) 706–717.
[8] A.S. Stillwell, D.C. Hoppock, M.E. Webber, Energy Recovery from Wastewater Treatment Plants in the United States: A Case Study of the Energy-Water Nexus, Sustainability 2 (2010) 945–962, https://doi.org/10.3390/su2040945.
[9] M. Uris, J.I. Linares, E. Arenas, Size optimization of a biomass-fired cogeneration plant CHP/CCHP (Combined heat and power/Combined heat, cooling and power) based on Organic Rankine Cycle for a district network in Spain, Energy 88 (2015) 935–945.
[10] E. Commission, REPowerEU: Joint European Action for more affordable, secure and sustainable energy, COM (2022) 108 final.
[11] C. Zhang, H. Su, J. Baeyens, T. Tan, Reviewing the anaerobic digestion of food waste for biogas production, Renew. Sustain. Energy Rev. 38 (2014) 383–392, https://doi.org/10.1016/j.rser.2014.05.038.
[12] L.N. Nguyen, J. Kumar, M.T. Vu, J.A.H. Mohammed, N. Pathak, A.S. Commault, D. Sutherland, J. Zdarta, V.K. Tyagi, L.D. Nghiem, Biomethane production from anaerobic co-digestion at wastewater treatment plants: A critical review on development and innovations in biogas upgrading techniques, Sci. Total Environ. 765 (2021), 142753, https://doi.org/10.1016/j.scitotenv.2020.142753.
[13] A. Feliu, X. Flotats, Renewable gases. An emerging energy Carrier. Fundación Naturgy, 2019 (in Spanish). Available online: https://www.fundacionnaturgy.org/publicacion/los-gases-renovables-un-vector-energetico-emergente/ (Accessed on 6 May 2021).
[14] W. Mo, Q. Zhang, Energy-nutrients-water nexus: integrated resource recovery in municipal wastewater treatment plants, J. Environ. Manage. 127 (2013) 255–267.
[15] P.L. McCarty, J. Bae, J. Kim, Domestic wastewater treatment as anet energy procucer.can thi be achieved? Environ. Sci. Technol. 45 (2011) 7100–7106.
[16] S.R. Qasim, Wastewater Treatment Plants: Planning, Design, and Operation, Routledge, 2017. ISBN 0-203-73420-3.
[17] G. Silvestre, B. Fernández, A. Bonmatí, Significance of Anaerobic Digestion as a Source of Clean Energy in Wastewater Treatment Plants, Energy Convers. Manage. 101 (2015) 255–262.
[18] S. Longo, B.M. d'Antoni, M. Bongards, A. Chaparro, A. Cronrath, F. Fatone, J. M. Lema, M. Mauricio-Iglesias, A. Soares, A. Hospido, Monitoring and Diagnosis of Energy Consumption in Wastewater Treatment Plants. A State of the Art and Proposals for Improvement, Appl. Energy 179 (2016) 1251–1268.
[19] Y. Zhang, H. Li, Energy Recovery from Wastewater Treatment Plants through Sludge Anaerobic Digestion: Effect of Low-Organic-Content Sludge, Environ. Sci. Pollut. Res. 26 (2019) 30544–30553.
[20] C. Morales-Polo, M.M. Cledera-Castro, An Optimized Water Reuse and Waste Valorization Method for a Sustainable Development of Poultry Slaughtering Plants, Desalin. Water Treat. 57 (2016) 2702–2711.
[21] D.J. Batstone, B. Virdis, The Role of Anaerobic Digestion in the Emerging Energy Economy, Curr. Opin. Biotechnol. 27 (2014) 142–149.
[22] G. Venkatesh, R.A. Elmi, Economic-Environmental Analysis of Handling Biogas from Sewage Sludge Digesters in WWTPs (Wastewater Treatment Plants) for Energy Recovery: Case Study of Bekkelaget WWTP in Oslo (Norway), Energy 58 (2013) 220–235.
[23] M. Horttanainen, J. Kaikko, R. Bergman, M. Pasila-Lehtinen, J. Nerg, Performance analysis of power generating sludge combustion plant and comparison against other sludge treatment technologies, Appl. Therm. Eng. 30 (2010) 110–118, https://doi.org/10.1016/j.applthermaleng.2009.07.005.
[24] N. Scarlat, J.-F. Dallemand, F. Fahl, Biogas: developments and perspectives in Europe, Renewable Energy 129 (2018) 457–472.
[25] C. Morales-Polo, M.M. Cledera-Castro, M. Revuelta-Aramburu, K. Hueso-Kortekaas, Bioconversion Process of Barley Crop Residues into Biogas—Energetic-Environmental Potential in Spain, Agronomy 11 (2021) 640.
[26] W. Balmant, B.H. Oliveira, D.A. Mitchell, J.V.C. Vargas, J.C. Ordonez, Optimal operating conditions for maximum biogas production in anaerobic bioreactors, Appl. Therm. Eng. 62 (2014) 197–206, https://doi.org/10.1016/j.applthermaleng.2013.09.033.
[27] C. Gallert, J. Winter, Mesophilic and thermophilic anaerobic digestion of source-sorted organic wastes: effect of ammonia on glucose degradation and methane production, Appl. Microbiol. Biotechnol. 48 (1997) 405–410, https://doi.org/10.1007/s002530051071.
[28] C. Morales-Polo, M.M. Cledera-Castro, K. Hueso-Kortekaas, M. Revuelta-Aramburu, Anaerobic Digestion in Wastewater Reactors of Separated Organic Fractions from Wholesale Markets Waste. Compositional and Batch Characterization. Energy and Environmental Feasibility, Sci. Total Environ. 726 (2020), 138567.
[29] C. Liu, Y. Sun, N. Li, B. Zhang, F. Zhen, Impact of temperature fluctuation on anaerobic fermentation process of upgrading bioreactor under solar radiant heating, Appl. Therm. Eng. 156 (2019) 382–391, https://doi.org/10.1016/j.applthermaleng.2019.04.092.
[30] A. González, J.R. Riba, A. Rius, Combined heat and power design based on environmental and cost criteria, Energy 116 (2016) 922–932, https://doi.org/10.1016/j.energy.2016.10.025.
[31] C. Cerezo-Dávila, C.F. Reinhart, J.L. Bemis, Modeling Boston: a workflow for the efficient generation and maintenance of urban building energy models from existing geospatial datasets, Energy 117 (2016) 237–250, https://doi.org/10.1016/j.energy.2016.10.057.
[32] M. Uris, J.I. Linares, E. Arenas, Feasibility assessment of an Organic Rankine Cycle (ORC) cogeneration plant (CHP/CCHP) fueled by biomass for a district network in mainland Spain, Energy 133 (2017) 969–985, https://doi.org/10.1016/j.energy.2017.05.160.
[33] A. Picardo, V.M. Soltero, M.E. Peralta, R. Chacartegui, District heating based on biogas from wastewater treatment plant, Energy 180 (2019) 649–664, https://doi.org/10.1016/j.energy.2019.05.123.
[34] J.F. García-Márquez, Biomethane production potential at Community of Madrid associated to integral water cycle, Graduated Thesis Disertation, School of Mines and Energy Engineering, Universidad Politécnica de Madrid, 2018 (in Spanish).

Available online: https://oa.upm.es/49614/1/PFG_Javier_Felix_Garcia_Marquez.pdf (Accessed on 13 May 2022).
[35] Y.A. Çengel, M.A. Boles, Thermodynamics, An Engineering Approach. Third Edition, McGraw-Hill (Boston), 1998.
[36] L. Goldstein, B. Hedman, D. Knowles, S.I. Freedman, R. Woods, T. Schweizer, Gas-Fired Distributed Energy Resource Technology Characterizations, NREL (NREL/TP-620-34783), November 2003. Available online: https://www.nrel.gov/docs/fy04osti/34783.pdf (Accessed on 5 May 2022).
[37] R. Barrella, I. Priego, J.I. Linares, E. Arenas, J.C. Romero, E. Centeno, Feasibility study of a centralised air source heat pump water heater to face energy poverty in block dwelllings in Madrid (Spain), Energies 13 (2020) 2723, https://doi.org/10.3390/en13112723.
[38] Ministry of Development, Ministry of Industry, Tourism and Trade (IDAE, Institute for Diversification and Saving of Energy), Energy performance scale. Existing buildings, 2011 (in Spanish). Available online: https://www.idae.es/uploads/documentos/documentos_11261_EscalaCalifEnerg_EdifExistentes_2011_accesible_c762988d.pdf (Accessed on 9 April 2020).
[39] DB-HE (MET files) (in Spanish). Available online: https://www.codigotecnico.org/images/stories/pdf/ahorroEnergia/CTEdatosMET_20140418.zip (Accessed on 9 April 2020).
[40] Building Technical Code, Basic Document HE (HE-1, Appendix D), April 2009 (in Spanish). Available online: https://www.codigotecnico.org/images/stories/pdf/ahorroEnergia/historico/DBHE_200801.pdf (Accessed on 9 April 2020).
[41] Ministry of Development, Ministry of Industry, Tourism and Trade (IDAE, Institute for Diversification and Saving of Energy), Energy performance scale. 2015 (in Spanish). Available online: https://energia.gob.es/desarrollo/EficienciaEnergetica/CertificacionEnergetica/DocumentosReconocidos/normativamodelosutilizacion/20151123-Calificacion-eficiencia-energetica-edificios.pdf (Accessed on 9 April 2020).
[42] Statistics National Institute, "Number of households according to household size and useful area of the dwelling", 2019 (in Spanish). Available online: https://www.ine.es/jaxi/Datos.htm?path=/t20/p274/serie/prov/p01/l0/&file=01006.px#!tabs-tabla (accessed 3 May 2021).
[43] A. Bejan, G. Tsatsaronis, M. Moran, Thermal Design & Optimization, John Wiley & Sons, New York, 1996.
[44] Nogawatio, Comparative analysis about usable technologies in residential building sector, SEDIGAS, 2017 (in Spanish). Available online: https://www.sedigas.es/php/download.php?f=paginas/338/archivos/2452/doc/es/EstudioTecnologiasResidencialEdificacion.pdf.
[45] A. Villanueva, Analysis of energy model of *Madrid Nuevo Norte*, carbon neutral, Proceedings of CONAMA 2020, May 31st – June 3rd, 2021 (in Spanish). (Accesed on 6 Mayo 2021).
[46] ROAMS. Available online: https://energia.roams.es/luz/tarifa/6-1/ (Accessed on 6 May 2021).